Original Article

doi: 10.16926/par.2026.14.08

Reactive Muscle Force Modulation Following Induced Belt Deceleration in Treadmill Gait

Rafał Borkowski [1ABCD], **Michalina Błażkiewicz** [12ABCD]

[1] Faculty of Rehabilitation, The Józef Piłsudski University of Physical Education in Warsaw, Warsaw, Poland
[2] Institute of Physical Culture Sciences, Jan Długosz University in Częstochowa, Częstochowa, Poland

Authors' Contribution: A – Study Design, B – Data Collection, C – Statistical Analysis, D – Manuscript Preparation, E – Funds Collection

Honorable Mention, Morecki & Fidelus Scientific Awards Competition in Biomechanics 2025

Abstract: Background: Gait stability requires rapid and coordinated neuromuscular responses to unexpected perturbations, yet the muscle-specific forces underlying reactive recovery remain poorly understood. The present study investigated changes in peak lower-limb muscle forces during the recovery step following treadmill belt decelerations applied in the pre-swing phase of the gait cycle in young, healthy females. Methods: Twenty-one participants completed treadmill walking trials with controlled unilateral belt decelerations while kinematic and kinetic data were recorded and processed using OpenSim musculoskeletal modeling to estimate individual muscle forces. Results: Across all examined muscles, peak muscle forces were higher during the recovery step compared to unperturbed walking, with the largest relative increases observed in the tensor fasciae latae (118.86%), iliacus (115.57%), and gluteus maximus (101.37%). Cluster analysis revealed a hierarchical response pattern: proximal hip stabilizers generated the greatest forces, intermediate muscles contributed to hip and ankle stabilization, and distal or postural muscles exhibited smaller adjustments. Conclusions: These results highlight the central role of hip and ankle musculature in restoring dynamic balance and support previous evidence on coordinated multi-muscle responses during reactive control. Furthermore, the findings indicate that effective recovery relies on sufficient muscle capacity across nearly all lower-limb muscles, emphasizing the potential importance of strength and power in balance interventions. Limitations of static optimization and treadmill-based perturbations are acknowledged, but relative changes in muscle forces provide robust insight into reactive control strategies. Overall, this study elucidates muscle-specific contributions to balance recovery following pre-swing deceleration, informing the design of targeted interventions for fall prevention and stability enhancement.

Keywords: Pre-swing perturbation; Lower-limb muscle forces; OpenSim

Corresponding author: Rafał Borkowski, email: rafal.borkowski@awf.edu.pl, Michalina Błażkiewicz, email: michalinablazkiewicz@awf.edu.pl

Recevied: 13.11.2025; Accepted: 21.11.2025; Published online: 7.01.2026

Citation: Borkowski R, Błażkiewicz M. Reactive Muscle Force Modulation Following Induced Belt Deceleration in Treadmill Gait. Phys Act Rev 2026; 14(1): 90-102. doi: 10.16926/par.2026.14.08

INTRODUCTION

Gait is considered the most fundamental and natural form of human locomotion [1]. Despite its apparent simplicity, it constitutes one of the most complex motor activities. The act of walking involves the repetitive and finely controlled loss and recovery of balance during alternating phases of support and swing, while simultaneously advancing the body's center of gravity in the forward direction. This dynamic process is mechanically demanding, as in the upright position, the human body behaves similarly to an inverted pendulum, requiring continuous adjustments to maintain equilibrium [2,3]. Consequently, maintaining stability in this posture poses a considerable challenge, particularly in the presence of external perturbations.

During walking, two primary forms of perturbations are typically distinguished: slips and trips [4]. A slip occurs when the frictional force required for forward progression exceeds the available friction between the walking surface and the foot [5]. Conversely, a trip takes place when the swing phase of the foot is disrupted due to insufficient ground clearance [6], often leading to a loss of balance and, in many cases, falls [7].

To counteract these perturbations, the human neuromuscular system engages a range of rapid and coordinated compensatory strategies [8]. Recovery from disturbance is achieved through adjustments in joint kinematics and kinetics, repositioning of the trunk, and corrective stepping responses collectively referred to as recovery steps [9]. The selection and execution of an appropriate strategy are governed by an intricate interaction between spinal and brainstem reflexes, task-dependent sensorimotor integration, and supraspinal control mechanisms that together regulate the timing, amplitude, and coordination of muscle responses [10]. The magnitude and direction of the perturbation further influence which compensatory strategy is adopted and how it is executed.

Reactions to gait perturbations have been extensively examined in previous research [11]. Beyond the analysis of kinematic, kinetic, and spatiotemporal parameters, particular attention has been devoted to muscle responses during recovery. Moreover, differences in reaction time, a key element in balance control and motor response initiation, were observed in populations with varying levels of physical activity, highlighting the importance of neuromotor abilities in adapting to sudden disturbances [12]. Beyond the analysis of kinematic, kinetic, and spatiotemporal parameters, particular attention has been devoted to muscle responses during recovery. Electromyography (EMG) has been the predominant technique used to explore the activation patterns of specific muscles [13]. However, EMG-based analyses have several notable limitations. First, only a limited number of muscles can be assessed simultaneously, restricting a comprehensive understanding of the muscle-specific coordination patterns involved in perturbation recovery. Second, EMG provides information about neural activation but not about the resulting muscle forces [14]. This distinction is critical, as the ability to generate adequate muscle force, rather than activation alone, ultimately determines the success of balance recovery.

A considerable portion of prior research has focused on older adults, given their increased susceptibility to falls [15]. Nonetheless, the examination of perturbation responses in young, healthy individuals remains essential. Studying this baseline population, free from age-related sensory decline, muscular weakness, or neurological impairment, enables a clearer understanding of the fundamental neuromuscular and biomechanical mechanisms underlying reactive balance control. In biomechanical analyses of responses to movement disorders, it is also important to consider limb dominance, as it affects postural symmetry and balance control, as demonstrated in recent studies of young adult populations [16]. Furthermore, defining normative characteristics of these mechanisms in young adults provides a valuable reference for comparison with

older or clinical populations. Such knowledge also contributes to the development of evidence-based interventions, including perturbation-based balance training programs, aimed at improving stability and preventing falls [17,18]. Analysis of muscle forces, particularly peak muscle forces, offers valuable insight into the mechanical demands imposed on individual muscles during reactive balance recovery. Unlike EMG, which reflects only the neural drive to the muscles, muscle force estimation integrates both neural and mechanical factors, such as muscle length, contraction velocity, and moment arm geometry, that together determine the actual output of the muscle-tendon unit [19-21]. Accordingly, the assessment of peak muscle forces allows for a more direct evaluation of the contributions of specific muscles to the compensatory response following perturbation [22]. Identifying which muscles experience the highest loads during recovery can further inform the design of targeted prevention and training strategies aimed at enhancing reactive stability and minimizing fall risk [23].

To date, studies directly examining the behavior of individual muscle forces during gait perturbation have been lacking [24]. Therefore, the present study aimed to investigate changes in peak lower-limb muscle forces during the recovery step following a perturbation, compared with those observed during unperturbed walking, in healthy young adults.

MATERIAL AND METHODS

Participant Characteristics and Ethical Approval

The sample size for the study was determined using G*Power 3.1.9.7 (University of Kiel, Germany) [25] based on an a priori Wilcoxon test. The parameters used for the calculation included a significance level (p) of 0.05, a desired statistical power of 0.80, and an effect size of 0.8, corresponding to a large effect. Based on these inputs, G*Power recommended a minimum sample size of 12 participants.

A total of twenty-one healthy young women took part in the study. Their mean age was 21.38 ± 1.32 years, with an average body mass of 61.38 ± 6.48 kg and an average height of 165.9 ± 4.53 cm. Participants were required to meet specific eligibility criteria: absence of any musculoskeletal or neurological disorders, no lower limb injuries within the preceding six months, engagement in recreational physical activity at least twice a week, and right-leg dominance [26,27]. Leg dominance was verified using the kicking test, in which participants identified the leg they would typically use to kick a ball. All participants were confirmed to be right-leg dominant.

Exclusion criteria included lack of prior treadmill-walking experience, self-reported balance difficulties, or use of medications known to affect nervous system function. Prior to inclusion in the study, all participants provided written informed consent. The research protocol was reviewed and approved by the University Institutional Review Board (SKE01-15/2023) and conducted in accordance with the ethical principles of the Declaration of Helsinki.

Trial and Perturbation Protocol

Kinematic (joint angles) and kinetic (joint torques and ground reaction forces) data for both perturbed and unperturbed gait were collected in the Interactive Gait Real-Time Analysis Laboratory (GRAIL, Motek Medical B.V., Amsterdam, The Netherlands). The GRAIL system included a dual-belt treadmill (2 × 500 mm width, 2200 mm length) operating at 1000 Hz, a ten-camera Vicon motion capture system (Bonita cameras; Vicon Metrics Ltd., Oxford, UK) recording at 100 Hz, three synchronized video cameras, and a 180° virtual reality projection screen (5 m diameter, 3 m height) supported by three projectors. All data were acquired and synchronized using D-Flow v. 3.26 software (Motek

Medical B.V., Amsterdam, The Netherlands), which was also employed for model calibration and the control of perturbations.

Upon arrival, participants' anthropometric measurements were recorded, and twenty-five reflective markers were placed on anatomical landmarks according to the Human Body Model 2 (HBM2) protocol (Figure 1). Participants wore their own comfortable athletic footwear, typically used for treadmill walking or gym activities. They were then positioned on the treadmill in a standardized T-pose to ensure precise alignment of the digital body model within D-Flow. A ceiling-mounted safety harness was used to secure participants and prevent falls throughout the trials.

Each participant completed a walking trial lasting 80 seconds, during which the treadmill speed was maintained at a constant 1.2 m/s. Within the trial, five perturbations were delivered at the 30th, 40th, 50th, 60th, and 70th seconds. Perturbations were set to level 5 on a scale of 1 to 5, corresponding to a sudden decrease in treadmill belt velocity of approximately 0.5 – 0.6 m/s. As a result, the speed of the left treadmill belt dropped to 0.6 – 0.7 m/s during perturbation events (Figure 2).

The perturbation protocol followed the methodology described by Sloot, et al. [28] and Chodkowska, et al. [24], with each perturbation lasting approximately 0.93 s. Perturbations were applied exclusively to the left treadmill belt, targeting the non-dominant (left) lower limb. The highest perturbation magnitude was selected to ensure a distinct and measurable response, allowing accurate estimation of peak joint and muscle loads. Perturbations were delivered during the Pre-Swing (PSw) phase of the gait cycle, corresponding to approximately 50 – 60% of the cycle as defined by Perry and Burnfield [29]. The D-Flow software enabled precise control of perturbation parameters, including magnitude, treadmill lane, timing, and event type. Since gait phases represent intervals rather than precise moments in time, a perturbation applied, for instance, at the 30th second during the PSw phase may correspond to slightly different points within the gait cycle across participants.

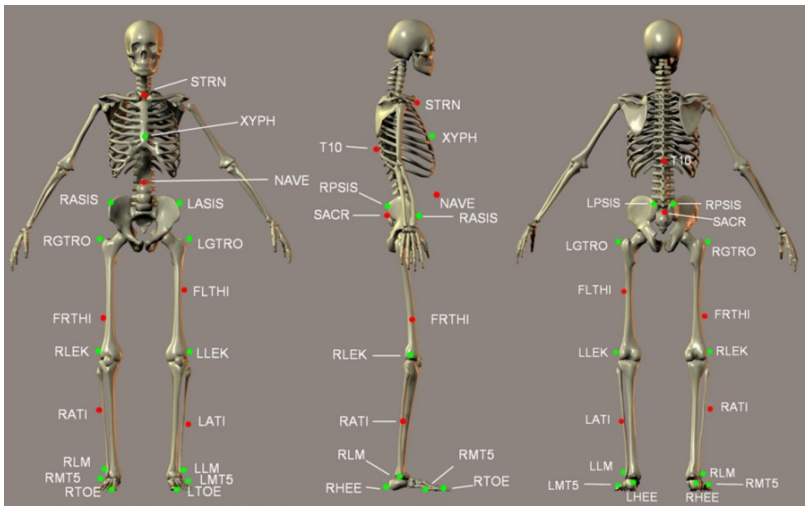

Figure 1. Front, lateral, and posterior views of the marker placement based on the Human Body Model 2. Green markers represent anatomical reference points used to define the skeletal model during initialization: STRN – jugular notch of the sternum; XYPH – xiphoid process; NAVE – navel; T10 – 10th thoracic vertebra; LASIS and RASIS – left and right anterior superior iliac spines; LPSIS and RPSIS – left and right posterior superior iliac spines; SACR – midpoint between LPSIS and RPSIS; LGTRO and RGTRO – left and right greater trochanters; LTHI and RTHI – left and right lateral thigh markers (midpoint between greater trochanter and lateral knee epicondyle); LLEK and RLEK – left and right lateral knee epicondyles; LSHK and RSHK – shank markers (midpoint between lateral knee and ankle malleolus); LLM and RLM – left and right lateral malleoli; LMT5 and RMT5 – fifth metatarsal heads; LTOE and RTOE – toe tips; LHEE and RHEE – heels.

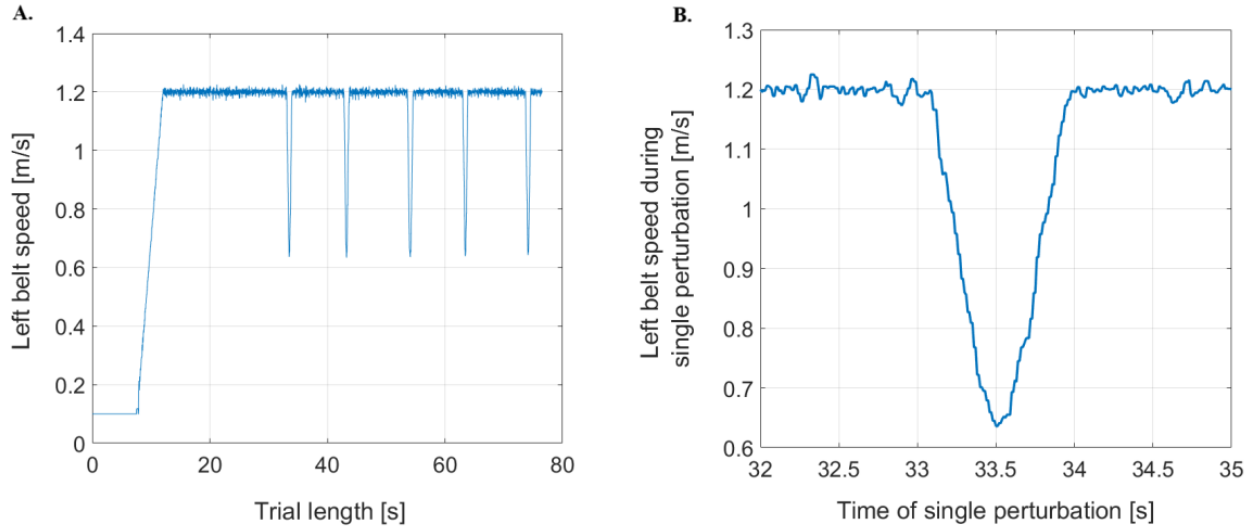

Figure 2. Left treadmill belt velocity: A. over the trial duration; B. detailed view of the first perturbation [24].

Data Processing

The musculoskeletal simulation process consisted of two main phases. In the first phase, motion and ground reaction force data were processed and converted into formats compatible with OpenSim v. 4.2. The processed data were used to perform musculoskeletal modeling and simulation, including model scaling, inverse kinematics, inverse dynamics, and static optimization to estimate muscle forces and joint kinetics.

In the second phase, following the completion of the musculoskeletal simulations, specific gait events and cycles were extracted for detailed analysis. This phase focused on identifying and isolating representative segments of both unperturbed and perturbed walking to enable direct comparison of gait mechanics under stable and disturbed conditions. The selection process was based on ground reaction force data, ensuring that each analyzed cycle accurately reflected consistent and repeatable walking behavior across participants.

Workflow for Musculoskeletal Simulation in OpenSim

In the first phase of data processing, motion data exported from D-Flow v3.26 were initially saved as *.mox files and imported into MATLAB 2021a (MathWorks, Natick, MA, USA) using a toolbox developed by Feldhege, et al. [30]. The imported data were then converted into OpenSim-compatible input files: *.trc files, containing three-dimensional marker trajectories captured during motion recording, and *.mot files, containing synchronized ground reaction force (GRF) and torque data [19]. Conversion scripts are available in public repository: https://github.com/RafalSci/Muscle-force-modulation-after-gait-perturbations.git.

For simulating muscle force contributions during both unperturbed walking and responses to perturbations, the Gait2392 musculoskeletal model (Fig. 3A), available in the OpenSim library, was used. This model is a three-dimensional, 23-degree-of-freedom representation of the human body comprising 92 musculotendon actuators, which represent 30 muscles controlling a single lower limb and 3 muscles acting on the torso on one side. The generic musculoskeletal model was then scaled to match each participant's anthropometry using the OpenSim Scale Tool. Scaling was performed based on static calibration trials to adjust segment lengths and marker placements, ensuring accurate correspondence with each participant's body geometry.

Following model scaling, inverse kinematics (IK) analysis was conducted to calculate joint angles across the trial. The IK algorithm aligns the model's virtual markers with experimentally recorded marker positions at each time frame, minimizing the sum of squared positional errors through a least-squares optimization approach. This process yields precise joint angle trajectories that describe three-dimensional limb and pelvis motion during both perturbed and unperturbed walking.

Inverse dynamics (ID) analysis was then performed to compute joint torques and joint reaction forces. This step applies Newton–Euler equations of motion to determine the net torques acting at each joint, based on the derived kinematic data, segment inertial properties, and external GRFs. The resulting joint torques provide insight into the mechanical demands imposed on the musculoskeletal system during normal gait and perturbation recovery, reflecting the total effort required to counteract internal and external forces.

In the final stage, static optimization (SO) was used to estimate individual muscle forces at each time frame. This algorithm distributes the net joint moments obtained from inverse dynamics among the model's muscles by minimizing the sum of squared muscle activations while satisfying physiological and mechanical constraints. The SO approach assumes quasi-static equilibrium at each instant of motion, allowing efficient computation of physiologically realistic muscle force patterns. Through this method, it was possible to identify which muscles contribute most significantly to maintaining stability and generating propulsion during perturbed gait (Fig. 3B).

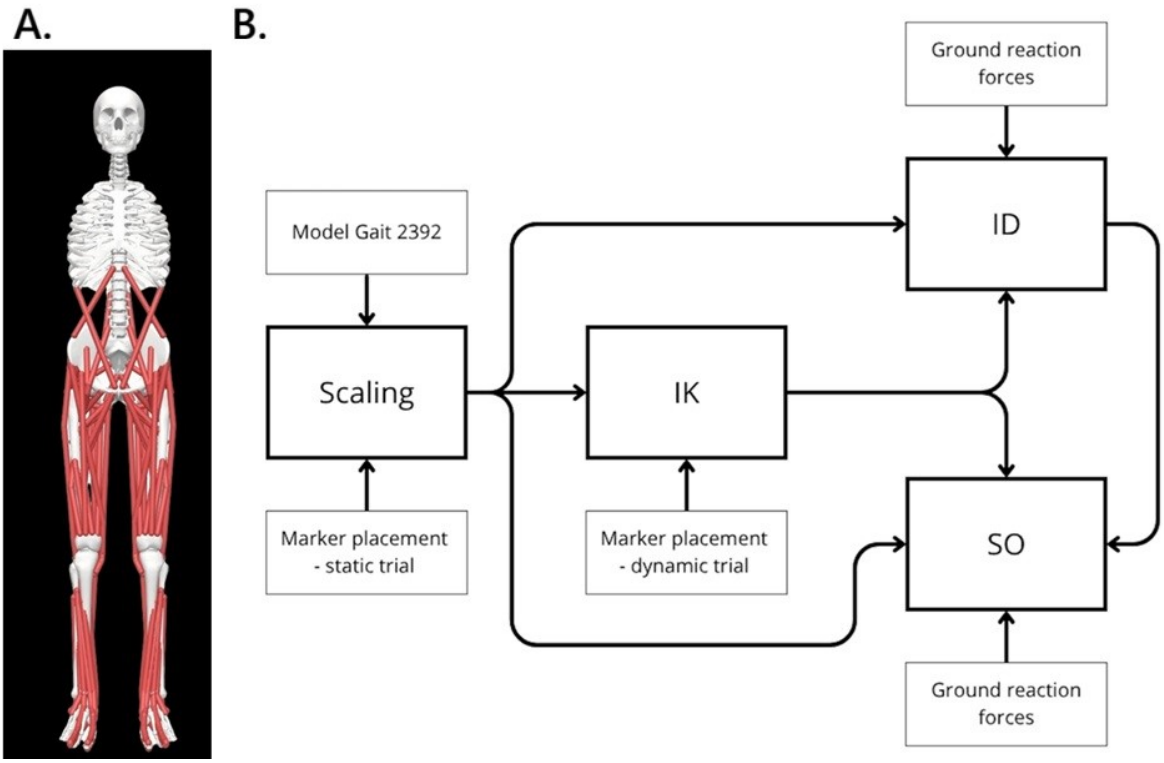

Figure 3. A. The Gait2392 model with 92 actuators representing 76 muscles, B. Schematic representation of the OpenSim data processing pipeline, illustrating sequential steps for model scaling, inverse kinematics (IK), inverse dynamics (ID), and static optimization (SO).

Data Extraction and Selection for Analysis

In this step, the recovery step and the unperturbed gait cycle were identified and isolated based on the vertical component of the ground reaction force (vGRF), which served to define the gait cycle boundaries. For both perturbed and unperturbed conditions, a gait cycle was defined as the interval between two consecutive ground contacts of the right foot.

The unperturbed gait cycle was defined as the tenth stride preceding the first perturbation, typically occurring around the 20th second of the trial, ensuring that participants maintained a stable and consistent walking pattern throughout the trial. The recovery step was identified as the response to the first perturbation applied to the left (non-dominant) lower limb, which occurred approximately at the 30th second of walking. This step was selected for analysis as it represented the most consistent and comparable reaction across participants.

In total, 21 unperturbed gait cycles of the right lower limb and 21 perturbed gait cycles corresponding to recovery steps following pre-swing (PSw) perturbations were included in the final analysis.

Statistical analysis

All statistical analyses were conducted using Statistica v.13 (Tibco StatSoft Inc., Tulsa, OK, USA) and comprised four sequential stages.

In the first stage, the peak muscle force (PMF) generated by each muscle during both the recovery step and unperturbed walking was identified. PMF was defined as the maximum muscle force value recorded within a single gait cycle.

In the second stage, the percentage difference in PMF between the recovery step and unperturbed walking was calculated for each muscle using the following equation:

$$D = \frac{F_{m\,rec.} - F_{m\,norm.}}{F_{m\,norm.}} \cdot 100\%$$

where $F_{m\,rec.}$ and $F_{m\,norm.}$ present the peak muscle forces during the recovery step and normal walking, respectively.

The third stage involved assessing the statistical significance of the observed differences. Based on the normality of distribution, as assessed by the Shapiro-Wilk test, the Wilcoxon signed-rank test was chosen. The level of significance was set at $p = 0.05$. Exact p-values were reported to four decimal places, and results with $p \leq 0.0001$ were presented as $p = 0.0001$. The effect size (r) was calculated using the formula: $r = \frac{Z}{\sqrt{N}}$, where Z is the standardized test statistic and N is the number of non-zero paired observations. Effect sizes were interpreted according to Cohen's guidelines (0.1 = small, 0.3 = medium, 0.5 = large) [31].

In the final stage, cluster analysis was performed to categorize the percentage differences in PMF into three distinct groups (n = 3) using the *k*-means algorithm. The Euclidean distance metric was applied, and the number of iterations was fixed at 50 to achieve an optimal balance between computational efficiency and clustering accuracy [32]. The resulting clusters were organized in tabular form, arranged from the largest to the smallest observed differences.

RESULTS

Across all examined muscles, peak muscle force (PMF) values recorded during the recovery step were higher compared to those observed during unperturbed walking. The

magnitude of these increases varied across muscles, ranging from 7.26% in the m. Peroneus brevis to 118.86% in the m. Tensor fasciae latae (Table 1).

Table 1. Median (lower and upper quartile) values of muscle forces during unperturbed gait and recovery step, with with percent differences and Wilcoxon test significance (* $p < 0.05$; ** $p < 0.001$) and Cohen's effect size (r). Color shading represents the magnitude of percentage changes, ranging from red for the largest differences, transitioning through orange and yellow for moderate changes, to green for the smallest differences.

Muscle	Unperturbet gait	Recovery step	Difference [%]	r
Cluster 1 (High response; ΔPMF ≥ 100%)				
Tensor fasciae latae	2.89 (1.83; 3.61)	5.78 (4.2; 7.97)	118.86 **	0.7926
Iliacus	9.06 (6.46; 12.37)	16.57 (13.73; 28.29)	115.57 **	0.8154
Gluteus maximus	2.32 (1.91; 2.98)	5.02 (4.4; 5.73)	101.37 **	0.8381
Cluster 2 (Moderate response; ΔPMF = 40 – 100%)				
Tibialis posterior	13.4 (7.7; 26.93)	28.41 (24.47; 32.65)	78.39 **	0.7168
Adductor brevis	6.65 (6.05; 9.59)	12.34 (11.25; 16.18)	75.33 **	0.8305
Pectineus	5.61 (3.53; 7.04)	9.43 (8.36; 12.2)	70.17 **	0.7926
Soleus	10.72 (6.24; 17.75)	20.43 (15.98; 23.5)	67.41 *	0.6940
Peroneus tertius	47.48 (36.2; 70.19)	79.2 (63.48; 99.63)	54 **	0.6409
Psoas minor and major	5.57 (4.73; 6.39)	7.73 (5.98; 11.02)	48.07 *	0.6030
Piriformis	5.67 (4.88; 6.2)	8.55 (7.42; 9.18)	47.43 **	0.7471
Biceps femoris	10.83 (9.8; 11.51)	16.51 (13.77; 18.47)	47.01 **	0.7471
Gluteus minimus	4.24 (3.73; 4.67)	5.63 (5.04; 6.73)	40.56 **	0.7547
Cluster 3 (Low response; ΔPMF ≤ 40%)				
Extensor digitorum	2.52 (2.28; 3.83)	4.03 (3.34; 4.41)	32.7 *	0.5726
Semitendinosus	13.09 (12.23; 14.94)	17.41 (16.16; 19.5)	31.15 **	0.7016
Internal oblique	34.21 (27.14; 43.51)	45.21 (40.9; 50.52)	30.01 *	0.7471
Flexor digitorum longus	24.73 (18.79; 31.05)	32.62 (28.26; 36.56)	29.83 *	0.7623
External oblique	14.39 (13.55; 17.21)	18.35 (16.43; 19.84)	28.39 *	0.5878
Gluteus medius	29.39 (26.82; 31.86)	38.88 (28.95; 42.77)	26.29 *	0.5802
Quadriceps femoris	3.28 (2.57; 3.45)	3.76 (3.24; 4.25)	25.98 *	0.5651
Semimembranosus	4.86 (4.24; 5.96)	6.16 (5.53; 6.86)	25.56 *	0.7016
Tibialis anterior	51.47 (28.91; 62.87)	62.25 (52.99; 65.88)	24.01	0.5044
Peroneus longus	6.55 (5.82; 6.74)	7.26 (6.87; 8.19)	21.57 **	0.7926
Quadratus femoris	20.62 (19.59; 22.88)	25.54 (23.21; 26.83)	21.04 **	0.8078
Gastrocnemius	18.57 (16.77; 21.43)	21.12 (19.96; 23.51)	19.2 *	0.5575
Gemellus	22.56 (20.71; 24.13)	26.41 (25.13; 27.33)	16.44 **	0.7926
Adductor magnus	21.73 (17.87; 24.7)	25.61 (23.38; 29.99)	16.27 *	0.5878
Extensor hallucis	8.59 (7.83; 10.07)	10.22 (9.07; 10.97)	13.25	0.4134
Flexor hallucis longus	14.86 (11.9; 16.03)	15.08 (13.9; 16.62)	10.82	0.3679
Sartorius	14.01 (12.82; 15.39)	15.17 (13.9; 16.99)	10.03 *	0.5044
Adductor longus	2.87 (2.72; 3.03)	3.2 (3.13; 3.34)	9.9 **	0.7395
Gracilis	4.75 (4.36; 5.42)	5.33 (5.14; 5.86)	9.62	0.4361
Erector spinae	3.71 (3.43; 3.88)	3.86 (3.59; 4.23)	9.19 *	0.6106
Peroneus brevis	31.66 (29.71; 32.32)	32.5 (30.29; 38.8)	7.26	0.3906

The k-means cluster analysis (n = 3) grouped muscles according to the magnitude of ΔPMF, revealing three distinct activation patterns. Cluster 1, representing high response (ΔPMF ≥ 100%), consisted of three muscles primarily responsible for proximal hip stabilization, with the largest increase observed in the Tensor fasciae latae (118.86%, $p < 0.001$) and the smallest in the Gluteus maximus (101.37%, $p < 0.001$). Cluster 2, representing moderate response (ΔPMF = 40 – 100%), included ten muscles contributing to hip and knee stabilization and lower-limb support, where the highest increase occurred in the Tibialis posterior (78.39%, $p < 0.001$) and the lowest in the Gluteus minimus (40.56%, $p < 0.001$). Cluster 3, representing low response (ΔPMF ≤ 40%), comprised 18 muscles, mainly distal or postural muscles, which exhibited smaller adjustments, with the highest increase seen in the Extensor digitorum (32.70%, $p < 0.05$) and the lowest in the Peroneus brevis (7.26%, not significant).

These findings indicate that recovery from a perturbation relies predominantly on proximal stabilizers and key lower-limb muscles, which generate the largest increases in force to rapidly restore balance. In contrast, distal and postural muscles show smaller adjustments, suggesting a hierarchical, coordinated neuromuscular strategy in which proximal muscles act as primary stabilizers while distal muscles provide fine-tuned support for postural control.

DISCUSSION

The present study investigated changes in peak muscle forces (PMF) during the recovery step in response to unexpected treadmill belt decelerations applied in the pre-swing (PSw) phase of the gait cycle in healthy young females using biomechanical modeling with OpenSim software. The main finding was a substantial increase in PMF across all lower-limb muscles, with the largest relative changes observed in the tensor fasciae latae (118.86%), iliacus (115.57%), and gluteus maximus (101.37%). These results highlight the critical role of hip musculature in restoring dynamic stability following sudden deceleration events and complement previous electromyographic and biomechanical evidence regarding multi-muscle coordination during reactive balance control [8,9,13,22].

The observed increases in PMF reflect the functional demands of reactive recovery. Muscles in the high-response cluster, primarily responsible for proximal hip stabilization, exhibited force increases exceeding 100%, indicating that these muscles are essential for rapid restoration of balance and trunk stabilization. Moderate increases (40–100%) were seen in muscles contributing to hip and knee stabilization, as well as lower-limb support, suggesting that these muscles act to maintain limb alignment and facilitate weight transfer during the compensatory step. Distal and postural muscles displayed smaller increases (<40%), indicating a supportive role in fine-tuning postural control rather than serving as the primary drivers of the corrective response. These results support a hierarchical neuromuscular strategy in which proximal muscles generate the largest forces, followed by intermediate stabilizers, with distal muscles providing secondary postural support [8,9,22].

The prominent involvement of hip muscles aligns with prior studies. Liu and Lockhart [33] emphasized the critical role of hip joint responses to perturbations in the sagittal plane. Similarly, in combat sports, the hip muscles and proximal segments play a key role in generating striking power and postural control, as confirmed by kinetic and EMG analyses performed during mae-geri kicks in Kyokushin karate [34]. Similarly, Namayeshi, et al. [35] reported that the gluteus maximus plays a major role in recovery from perturbations applied during the initial contact phase. Shokouhi, et al. [36] also highlighted the importance of hip muscles, noting significant increases in positive work (concentric

contractions) of hip musculature, although they identified the knee joint as the main contributor to negative leg work (eccentric energy absorption). In the present study, most knee muscles, except for the biceps femoris, were grouped in the low-response cluster, likely reflecting the different timing of perturbation application, which occurred during the PSw phase rather than immediately after heel strike.

The second cluster, showing moderate increases, mainly included muscles stabilizing the hip and ankle joints [37,38]. This underscores the importance of coordinated hip and ankle stabilization in response to sudden deceleration. Asghari, et al. [39] demonstrated that both hip and ankle stabilizing muscles play a vital role in balance recovery after gait perturbations, while Namayeshi, et al. [40] highlighted the critical contribution of ankle plantarflexors and the importance of their activation timing for successful recovery in young adults. The observed increases in PMFs of the soleus and tibialis posterior in the present paper further support the role of ankle muscles in reactive balance control.

The results also indicate that successful execution of the recovery step requires a muscle strength surplus across nearly all lower-limb muscles. This aligns with the conclusions of Sherrington, et al. [23], who emphasized the importance of resistance exercises in fall prevention programs for older adults, although the evidence was of moderate certainty. Notably, improvements in proprioception induced by resistance training [41] complicate the attribution of fall prevention solely to increased muscle strength. Moreover, some studies suggest that the ability to generate rapid muscle power may be more critical than maximal strength for effective perturbation recovery [42], highlighting the need for further research on the relative contributions of strength and power.

The use of static optimization in OpenSim allowed efficient estimation of individual muscle forces but introduced limitations, particularly regarding antagonist co-contraction and tendon compliance. Methodological evaluations suggest that static optimization may underestimate antagonist activity, potentially underrepresenting the forces generated by co-stabilizing muscles [43]. However, the relative PMF changes observed here are generally robust to these limitations and provide reliable insight into the direction and magnitude of muscle response adaptations.

Finally, the study population consisted of young, physically active females, providing insight into optimal neuromuscular control. Caution is warranted in generalizing these findings to older adults or clinical populations. Similarly, treadmill-based decelerations, while highly controlled, differ from overground perturbations in sensory feedback and task demands [44]. Nonetheless, split-belt perturbations are validated proxies for studying reactive stepping mechanics in repeatable laboratory conditions [44].

CONCLUSION

In summary, the recovery step following a treadmill belt deceleration in the pre-swing phase involves a graded, muscle-specific response, with proximal hip stabilizers generating the largest forces, intermediate stabilizers contributing to hip and ankle joint control, and distal or postural muscles providing fine-tuned postural support. These findings enhance our understanding of neuromuscular coordination during reactive balance and have important implications for designing targeted interventions to improve stability and reduce fall risk.

Funding Statement: This research received no external funding.

Conflicts of Interest: The authors declare no conflict of interest.

REFERENCES

1. Winter DA. Human balance and posture control during standing and walking. Gait Posture 1995; 3: 193-214. doi: 10.1016/0966-6362(96)82849-9
2. Horak FB. Postural orientation and equilibrium: what do we need to know about neural control of balance to prevent falls? Age Ageing 2006; 35(Suppl 2): ii7-ii11. doi: 10.1093/ageing/afl077
3. Horak FB, Nashner LM. Central programming of postural movements: adaptation to altered support-surface configurations. J Neurophysiol 1986; 55: 1369-1381. doi: 10.1152/jn.1986.55.6.1369
4. Yoo D, Seo KH, Lee BC. The effect of the most common gait perturbations on the compensatory limb's ankle, knee, and hip moments during the first stepping response. Gait Posture 2019; 71: 98-104. doi: 10.1016/j.gaitpost.2019.04.013
5. Hanson JP, Redfern MS, Mazumdar M. Predicting slips and falls considering required and available friction. Ergonomics 1999; 42: 1619-1633. doi: 10.1080/001401399184712
6. Chang WR, Leclercq S, Lockhart TE, Haslam R. State of science: occupational slips, trips and falls on the same level. Ergonomics 2016; 59: 861-883. doi: 10.1080/00140139.2016.1157214
7. Robinovitch SN, Feldman F, Yang Y, Schonnop R, Leung PM, Sarraf T, et al. Video capture of the circumstances of falls in elderly people residing in long-term care: an observational study. Lancet 2013; 381: 47-54. doi: 10.1016/S0140-6736(12)61263-X
8. Rogers MW, Mille ML. Balance perturbations. Handb Clin Neurol 2018; 159: 85-105. doi: 10.1016/B978-0-444-63916-5.00005-7
9. Dusane S, Bhatt T. Can prior exposure to repeated non-paretic slips improve reactive responses on novel paretic slips among people with chronic stroke? Exp Brain Res 2022; 240: 1069-1080. doi: 10.1007/s00221-021-06300-8
10. Bhatt T, Patel P, Dusane S, DelDonno SR, Langenecker SA. Neural mechanisms involved in mental imagery of slip-perturbation while walking: a preliminary fMRI study. Front Behav Neurosci 2018; 12: 203. doi: 10.3389/fnbeh.2018.00203
11. Chodkowska K, Borkowski R, Błażkiewicz M. Perturbations during gait on a split-belt treadmill: a scoping review. Appl Sci 2024; 14: 9852. doi: 10.3390/app14219852
12. Berdowska A, Dusiński D, Bandurska K, Tsos A. Effort and reaction time in weightlifters, manual workers, and students – a pilot study. Phys Act Rev 2025; 13(1): 97-105. doi: 10.16926/par.2025.13.09
13. Taylor Z, Walsh GS, Hawkins H, Inacio M, Esser P. Perturbations during gait: a systematic review of methodologies and outcomes. Sensors 2022; 22: 5927. doi: 10.3390/s22155927
14. Vigotsky AD, Halperin I, Lehman GJ, Trajano GS, Vieira TM. Interpreting signal amplitudes in surface electromyography studies in sport and rehabilitation sciences. Front Physiol 2017; 8: 985. doi: 10.3389/fphys.2017.00985
15. Aprigliano F, Monaco V, Tropea P, Martelli D, Vitiello N, Micera S. Effectiveness of a robot-mediated strategy while counteracting multidirectional slippages. Robotica 2019; 37: 2119-2131. doi: 10.1017/S0263574719000626
16. Hadamus A, Gulatowska M, Ferenc A, Shahnazaryan K, Brzuszkiewicz-Kuźmicka G, Błażkiewicz M. Influence of leg dominance on the symmetry in body balance measurements. Phys Act Rev 2025; 13: 88-96. doi: 10.16926/par.2025.13.08
17. Sharma S, Szabo I-Z, Danielsen M, Andersen S, Nørgaard J, Lord S, et al. Perturbation-based balance training improves reactive balance and reduces falls in older people: a systematic review and meta-analysis; 2025.
18. Okubo Y, Brodie MA, Sturnieks DL, Hicks C, Lord SR. A pilot study of reactive balance training using trips and slips with increasing unpredictability in young and older adults. Clin Biomech 2019; 67: 171-179. doi: 10.1016/j.clinbiomech.2019.05.016
19. Delp SL, Anderson FC, Arnold AS, Loan P, Habib A, John CT, et al. OpenSim: open-source software to create and analyze dynamic simulations of movement. IEEE Trans Biomed Eng 2007; 54: 1940-1950. doi: 10.1109/TBME.2007.901024
20. Arnold EM, Ward SR, Lieber RL, Delp SL. A model of the lower limb for analysis of human movement. Ann Biomed Eng 2010; 38: 269-279. doi: 10.1007/s10439-009-9852-5
21. Millard M, Uchida T, Seth A, Delp SL. Flexing computational muscle: modeling and simulation of musculotendon dynamics. J Biomech Eng 2013; 135: 021005. doi: 10.1115/1.4023390

22. Seth A, Hicks JL, Uchida TK, Habib A, Dembia CL, Dunne JJ, et al. OpenSim: simulating musculoskeletal dynamics and neuromuscular control to study human and animal movement. PLoS Comput Biol 2018; 14: e1006223. doi: 10.1371/journal.pcbi.1006223
23. Sherrington C, Fairhall N, Wallbank G, Tiedemann A, Michaleff ZA, Howard K, et al. Exercise for preventing falls in older people living in the community: an abridged Cochrane systematic review. Br J Sports Med 2020; 54: 885-891. doi: 10.1136/bjsports-2019-101512
24. Chodkowska K, Błażkiewicz M, Kędziorek J, Ortenburger D, Wąsik J. How does induced deceleration of one treadmill belt in the pre-swing gait phase change gait pattern? Appl Sci 2024; 14: 11456.
25. Faul F, Erdfelder E, Lang AG, Buchner A. G*Power 3: a flexible statistical power analysis program for the social, behavioral, and biomedical sciences. Behav Res Methods 2007; 39: 175-191. doi: 10.3758/BF03193146
26. Promsri A, Bangkomdet K, Jindatham I, Jenchang T. Leg dominance–surface stability interaction: effects on postural control assessed by smartphone-based accelerometry. Sports 2023; 11: 75. doi: 10.3390/sports11040075
27. Promsri A, Haid T, Federolf P. How does lower limb dominance influence postural control movements during single-leg stance? Hum Mov Sci 2018; 58: 165-174. doi: 10.1016/j.humov.2018.02.003
28. Sloot LH, van den Noort JC, van der Krogt MM, Bruijn SM, Harlaar J. Can treadmill perturbations evoke stretch reflexes in the calf muscles? PLoS One 2015; 10: e0144815. doi: 10.1371/journal.pone.0144815
29. Perry J, Burnfield JM. Gait analysis: normal and pathological function. 2nd ed. California: Slack; 2010.
30. Feldhege F, Richter K, Bruhn S, Fischer DC, Mittlmeier T. MATLAB-based tools for automated processing of motion tracking data provided by the GRAIL. Gait Posture 2021; 90: 422-426. doi: 10.1016/j.gaitpost.2021.09.179
31. Cohen J. Statistical power analysis for the behavioral sciences. 2nd ed.; 1988.
32. Ahmed M, Seraj R, Islam SM. The k-means algorithm: a comprehensive survey and performance evaluation. Electronics 2020; 9: 1295. doi: 10.3390/electronics9081295
33. Liu J, Lockhart TE. Age-related joint moment characteristics during normal gait and successful reactive-recovery from unexpected slip perturbations. Gait Posture 2009; 30: 276-281. doi: 10.1016/j.gaitpost.2009.04.005
34. Mosler D, Góra T, Kaczmarski J, Błaszczyszyn M, Chociaj M, Borysiuk Z. Target kinematic effect in Kyokushin karate front kicks. Phys Act Rev 2025; 13: 156-166. doi: 10.16926/par.2025.13.14
35. Namayeshi T, Lee PVS, Ackland D. Gait balance recovery after tripping: influence of walking speed and ground inclination on muscle and joint function. J Biomech 2024; 172: 112178. doi: 10.1016/j.jbiomech.2024.112178
36. Shokouhi S, Mokhtarzadeh H, Lee PV. Lower extremity joint power and work during recovery following trip-induced perturbations. Gait Posture 2024; 107: 1-7. doi: 10.1016/j.gaitpost.2023.09.005
37. Parvaresh KC, Chang C, Patel A, Lieber RL, Ball ST, Ward SR. Architecture of the short external rotator muscles of the hip. BMC Musculoskelet Disord 2019; 20: 611. doi: 10.1186/s12891-019-2995-0
38. Feger MA, Donovan L, Hart JM, Hertel J. Lower extremity muscle activation during functional exercises in patients with and without chronic ankle instability. PM R 2014; 6: 602-611. doi: 10.1016/j.pmrj.2013.12.013
39. Asghari M, Elali K, Sullivan A, LaFleur B, Madigan ML, Toosizadeh N. Assessing the role of ankle and hip joint proprioceptive information in balance recovery using vibratory stimulation. Heliyon 2024; 10: e25979. doi: 10.1016/j.heliyon.2024.e25979
40. Namayeshi T, Haddara R, Ackland D, Lee PVS. The role of the ankle plantar flexor muscles in trip recovery during walking: a computational modeling study. Front Sports Act Living 2023; 5: 1153229. doi: 10.3389/fspor.2023.1153229
41. Guede-Rojas F, Benavides-Villanueva A, Salgado-González S, Mendoza C, Arias-Álvarez G, Soto-Martínez A, et al. Effect of strength training on knee proprioception in patients with knee osteoarthritis: a systematic review and meta-analysis. Sports Med Health Sci 2024; 6: 101-110. doi: 10.1016/j.smhs.2023.10.005
42. Simpkins C, Yang F. Muscle power is more important than strength in preventing falls in community-dwelling older adults. J Biomech 2022; 134: 111018. doi: 10.1016/j.jbiomech.2022.111018
43. Kian A, Pizzolato C, Halaki M, Ginn K, Lloyd D, Reed D, et al. Static optimization underestimates antagonist muscle activity at the glenohumeral joint: a musculoskeletal modeling study. J Biomech 2019; 97: 109348. doi: 10.1016/j.jbiomech.2019.109348

44. Siragy T, Russo Y, Young W, Lamb SE. Comparison of over-ground and treadmill perturbations for simulation of real-world slips and trips: a systematic review. Gait Posture 2023; 100: 201-209. doi: 10.1016/j.gaitpost.2022.12.015